ELSEVIER

Journal of Nuclear Materials 295 (2001) 273–280

journal of nuclear materials

www.elsevier.nl/locate/jnucmat

Effects of phosphorus on defects accumulation and annealing in electron-irradiated Fe–Ni austenitic alloys

V.L. Arbuzov *, A.P. Druzhkov, S.E. Danilov

Institute of Metal Physics, Ural Branch Russian Academy of Sciences, 18 S. Kovalevskaya St., 620219, Ekaterinburg, GSP-170 Russian Federation

Received 26 October 2000; accepted 7 February 2001

Abstract

Pure austenitic alloy Fe–36% Ni and the same alloy doped with phosphorus (0.1% P) were irradiated with 5 MeV electrons at different temperatures (270–573 K). Using the methods of positron annihilation and residual resistivity it was shown that at the irradiation temperature of 270 K vacancies are mobile in both alloys and form vacancy clusters. In Fe–36Ni–0.1P alloy vacancy clusters are decorated with phosphorus atoms. After the irradiation at 423 K the decoration effect is not observed. At the irradiation temperature of 573 K the addition of phosphorus results in the suppression of vacancy supersaturation. A conclusion is made that, at the elevated irradiation temperatures, suppression of vacancy supersaturation occurs due to the interstitial–phosphorus interaction.

PACS: 61.72.Ji; 78.70.Bj; S1.2

1. Introduction

Addition of small amounts of different elements modifies the properties of nuclear reactor structural materials. Alloying is one of the effective ways to improve their radiation resistance. It is known [1] that such impurities as C, P, Ti affect the behavior of swelling and creep of austenitic alloys. For example, the addition of phosphorus in the amount of 0.01 wt% and higher into type 316 stainless steel strongly suppresses void swelling [2].

However the factors suppressing the void development, and those decreasing vacancy supersaturation in the presence of phosphorus addition, have not been elucidated to the full extent.

There are three main causes of phosphorus effect which have been discussed in the literature:

1. It has been shown in [3] that during the irradiation of austenitic steels there takes place radiation-induced formation of phosphides Fe_2P. It is hypothesized that these serve as effective sinks for point defects.
2. Garner et al. [4] point out that phosphorus in austenitic alloys presents a fast-diffusing impurity leading to an increase of the effective diffusion coefficient of vacancies, and correspondingly, to a decrease of supersaturation of vacancies.
3. It has been suggested in [5,6] that phosphorus atoms in austenitic alloys strongly interact both with the interstitials and the vacancies. A conclusion is made that phosphorus atoms, on the contrary, reduce the mobility of vacancies. In the opinion of the authors of [5,6], long-range migration of vacancies in phosphorus-doped austenitic alloys occurs at temperatures above 573 K. It should be noted that the authors performed the in situ irradiation and investigations under a high-voltage electron microscope and monitored the behavior of large defect clusters such as interstitial-type dislocation loops, vacancy loops and stacking fault tetrahedra.

The purpose of this paper is the investigation of the behavior of vacancies, the initial stage of vacancy cluster nucleation under electron irradiation and their evolution

* Corresponding author. Tel.: +7-3432 499 038; fax: +7-3432 740 003.

E-mail address: arbuzov@imp.uran.ru (V.L. Arbuzov).

0022-3115/01/$ - see front matter
PII: S0022-3115(01)00505-0

in the process of annealing in model austenitic alloys Fe–36 wt% Ni with phosphorus addition. To find out the effect of phosphorus on these processes and the probable causes of void swelling suppression, the methods of positron annihilation and residual electrical resistivity were used. Positrons are trapped in vacancies and vacancy clusters, not responding in the same way to interstitial atoms (IA) and their agglomerates [7].

In the present work, use was also made of a recently proposed technique [8,9] of identification of the impurity atoms decorating the vacancies by the data on positron–core electron annihilation. This technique has been tested earlier in our investigations of the interaction between vacancies and phosphorus atoms in nickel [10].

Residual electrical resistivity in austenitic alloys is highly sensitive to the processes of short-range ordering [11] induced by the migration of point defects and other structural-phase transformations in these alloys.

2. Experimental aspects

Alloys of Fe–36 wt% Ni (Fe–Ni) were prepared from high-purity iron and nickel. After rolling, cutting and electrical polishing, the samples were annealed under 10^{-6} Pa vacuum at 1323 K during 15 h for homogenizing, and then quickly cooled ($\sim$100 K/s). The presence of one austenitic phase in the samples was checked by X-ray analysis.

Part of the Fe–Ni samples was saturated with phosphorus from gaseous phase in a closed quartz volume evacuated to 10^{-6} Pa at 1323 K during 18 h, with subsequent fast cooling. Phosphorus concentration was $\sim$0.1 at.%.

Samples were irradiated at 270, 423 and 573 K with 5 MeV electrons on a linear accelerator.

After irradiation the samples underwent annealing both in a pure helium atmosphere, and under vacuum (10^{-6} Pa) at 270 to 900 K during 25 min in step of 25 K (with the average temperature rise rate of 1 K/min).

A standard potentiometric method with the measurement error of 0.02% was used to measure the residual electrical resistivity. A one-dimensional angular correlation annihilation radiation (ACAR) spectrometer with a resolution of 1 mrad $\times$ 160 mrad was used [10]. The ACAR spectra represent coincidence count rate $N(\theta)$ as a function of angle θ. Angle $\theta = p_z/m_0c$, where p_z is projection of the electron–positron momentum on axis z, m_0 is the electron stationary mass, and c is the velocity of light. The ACAR experiments allow information to be obtained about momentum distribution of annihilating electrons [10]. It is possible to separate the inputs from annihilation of positrons with the almost free electrons (low-momentum spectrum part) and the core electrons (high-momentum spectrum part). The lattice crystalline field has little effect on the strong-fixed electrons, and thus the high-momentum part of the ACAR spectrum carries information about the type of atoms in the region of positron annihilation.

In characterizing the changes in the shape of ACAR spectra due to positron trapping by defects, use was made of S- and W-parameters [10]. The S- and W-parameters were defined as a ratio of the sum of coincidence count rates in the range of angles θ from 0 to 3.5 mrad and from 10 to 15 mrad to full coincidence count rate of ACAR spectrum, respectively. The S-parameter characterizes the probability of positron annihilation with the almost free electrons, and the W-parameter, with the core electrons.

In the general case, positrons in the sample annihilate both from the trapped and the free states. In case of positrons being trapped by one type of defects, e.g., monovacancies, the S-parameter (and the W-parameter, similarly) is linked with monovacancy concentration C_v through the relationship [12]

$$S = (\lambda_f S_f + \mu_v C_v S_v)/(\lambda_f + \mu_v C_v), \quad (1)$$

where λ_f is the rate of positron annihilation in a free state; μ_v is the specific trapping rate; S_f, S_v are parameter values for the cases where positrons annihilate from the free and the trapped states, respectively.For defect type analysis, the R-parameter was also used, presenting a combination of the S- and W-parameters [10]:

$$R = |(S - S_f)/(W - W_f)|. \quad (2)$$

The R-parameter does not depend on the defect concentration, but is determined by their type. The values of the R-parameter for the three-dimensional clusters, monovacancies and vacancy loops are related to one another as $R_c > R_V > R_{vl}$ [13].

3. Experimental results

3.1. Positron annihilation

3.1.1. Annihilation parameters as a function of the electron fluence

In the initial state (before irradiation), annihilation parameters in Fe–Ni and Fe–Ni–P alloys coincide and are close to parameters of pure nickel. Let us consider the result of the irradiation of Fe–Ni alloy. The dependence of S-parameter on the electron fluence at the irradiation temperatures of 270, 423 and 573 K is illustrated in Fig. 1(a). The growth of S-parameter with the increase of the fluence is observed for all the irradiation temperatures. The most intensive growth is characteristic of 270 K. At the irradiation with the fluence over 2×10^{22} m^{-2}, the S-parameter exceeds the level of S_v, which characterizes the annihilation of

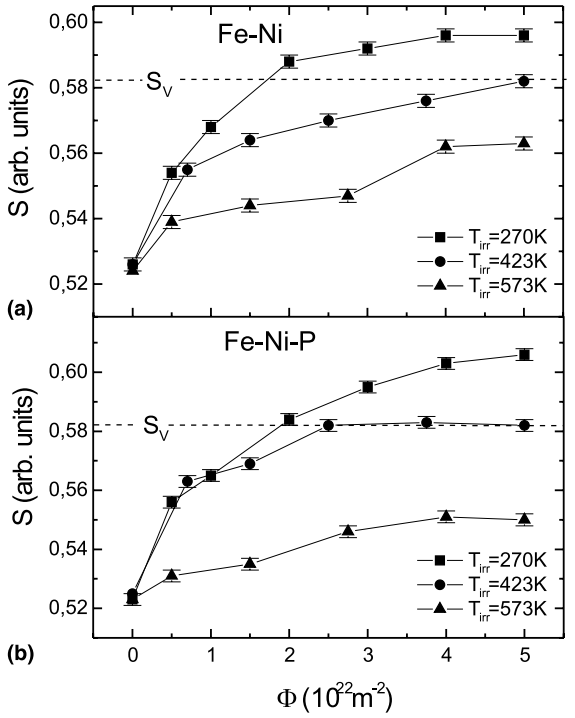

Fig. 1. *S*-parameter variation versus irradiation fluence at 270, 423, 573 K in Fe–Ni (a) and Fe–Ni–P (b) austenitic alloys, respectively.

positrons from the entrapped states by monovacancies in nickel [14], and continues growing with the fluence growth. As expression (1) shows, the *S*-parameter depends on specific trapping rate μ_v, value of S_v, and monovacancy concentration. There is no physical ground to suppose that for Fe–Ni the values of μ_v and S_v would differ substantially from similar values for Ni. The fcc electronic structures of Fe–Ni and Ni are practically identical, which is proved by the close values of the annihilation parameters in the initial state. Correspondingly, the value of S_v in the alloy must not differ from S_v in Ni.

The accumulation rate of vacancies in Fe–Ni alloy may be much higher than that in Ni due to lower mobility of IA and lower probability of their recombination with vacancies. It is known that in austenitic Fe–Cr–Ni alloys the migration energy of IAs is 0.9 eV, and in Ni it is 0.15 eV [11,15]. However, higher monovacancy concentration cannot ensure *S*-parameter growth in excess of S_v. Evidently, *S*-parameter growth above the value of S_v is connected with vacancy migration and formation of vacancy clusters of three-dimensional configuration. It is well known [12] that in the case of positron capture by three-dimensional clusters, *S*-parameter reaches the values higher than S_v. Thus at the irradiation temperature of 270 K, vacancies in Fe–Ni alloy are already mobile and form three-dimensional clusters, similar to Fe–Cr–Ni alloys [7].

With the increase of the irradiation temperature, values of *S*-parameter decrease (Fig. 1(a)). It is clear that with the increase of the irradiation temperature, mobility of the IA and vacancy also increases, resulting in either their more intensive mutual recombination, or annihilation on sinks [16]. Respectively, the concentration of vacancy-type defects preserved in the samples decreases with the irradiation temperature rise. The irradiation temperature rise is also accompanied with the change in the structure of the accumulated defects, which may be judged upon by the *R*-parameter drop. For example, for a fluence of 5×10^{22} m^{-2} at $T_{irr} = 270$ K, $R = 2.80 \pm 0.18$, while at $T_{irr} = 573$ K, $R = 2.37 \pm 0.13$, which may be due to the prevailing formation of two-dimensional clusters with the increase of the irradiation temperature.

Let us consider the data on the accumulation of vacancy-type defects in Fe–Ni–P alloy as shown in Fig. 1(b). Vacancy clustering under low-temperature irradiation (at 270 K) also occurs in the doped Fe–Ni–P alloy. However, the *S*-parameter reaches the values higher than that in Fe–Ni, and values of the *R*-parameter in Fe–Ni–P differ from those in Fe–Ni under low-temperature irradiation (Fig. 2). It may be seen from Fig. 2 that in both alloys the *R*-parameter does not depend on the electron fluence; however, in the phosphorus-doped alloy the *R*-parameter values are lower. Thus phosphorus exerts substantial influence on the structure of vacancy clusters formed at the irradiation temperature of 270 K.

With the irradiation temperature rise, similar to the case of Fe–Ni, concentration of the accumulated vacancy-type defects drops. After the irradiation at 573 K, however, the values of *S*-parameter in Fe–Ni–P are considerably lower than those in Fe–Ni.

One more circumstance should be noted. As may be seen in Fig. 1, the rate of *S*-parameter growth with the increase of the electron fluence slows down in both alloys irrespective of the temperature of irradiation, i.e.,

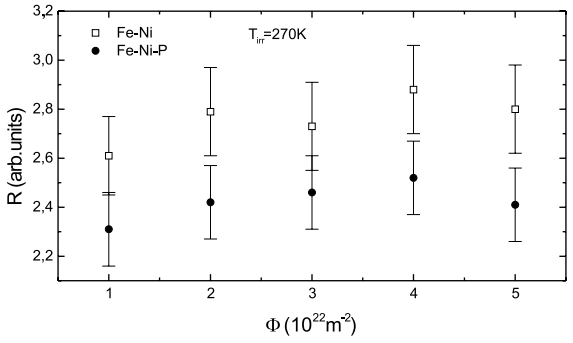

Fig. 2. *R*-parameter variation versus irradiation fluence at 270 K in Fe–Ni and Fe–Ni–P alloys.

tends to the state of saturation. The state of saturation may occur for two reasons: (1) The concentration of positron capture centers has reached $\approx 10^{-4}$ per atom. (2) A quasi-stationary state has set, at which the defect concentration and structure vary but slightly with the increase of fluence. The first reason works for the irradiation at 270 K only. It may therefore be supposed that, after the irradiation of a fluence of $3–4 \times 10^{22}$ m^{-2}, a quasi-stationary state of the defect structure is reached.

3.1.2. Behavior of annihilation parameters in the course of annealing

Let us consider the behavior of annihilation parameters in the course of the isochronal annealing of irradiated samples. The variations of *S*-parameter as a function of the isochronal annealing temperature for Fe–Ni alloy irradiated to a fluence of 5×10^{22} m^{-2} at 270, 423 and 573 K, respectively, are shown in Fig. 3(a). Let us first look into the results of annealing of the sample irradiated at 270 K. As may be seen in Fig. 3(a), the *S*-parameter remains constant until 420 K, then it decreases continuously. At 860 K the *S*-parameter reaches its initial value. At that, at temperatures over

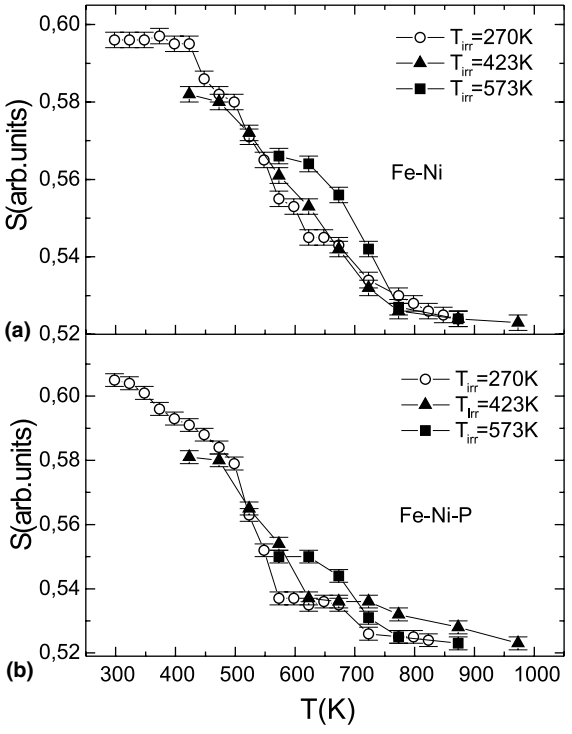

Fig. 3. Evolution of the *S*-parameter as a function of the isochronal annealing temperature in 5×10^{22} m^{-2} electron-irradiated Fe–Ni (a) and Fe–Ni–P (b) at 270, 423, 573 K, respectively.

600 K, the *R*-parameter drops to 2.39 ± 0.13 thus testifying to formation of two-dimensional clusters – the vacancy loop centers. The *S*-parameter behavior after the irradiation at 423 K differs noticeably from that at 270 K. Different behavior of the *S*-parameter is observed after the irradiation at 573 K. The *S*-parameter decrease starts at a temperature above 650 K. As has been noted in Section 3.1.1, the *R*-parameter value after the same irradiation is the lowest, that is, already in the process of the irradiation there goes formation of two-dimensional vacancy clusters. Such a configuration is more thermally stable, and this fact affects the mechanism of their annealing.

The dependence of *S*-parameter on the isochronal annealing for Fe–Ni–P alloy irradiated at different temperatures is presented in Fig. 3(b). Let us consider the results of annealing of a sample irradiated at 270 K. As distinct from Fe–Ni, *S*-parameter decrease in this alloy starts at 340 K, being slow in the beginning, and becoming faster over 500 K. By 600 K, the *S*-parameter reaches a value lower than that in the Fe–Ni alloy. In the range between 600 and 700 K of the temperature dependence curve of *S*-parameter, a distinct plateau is observed. Regretfully, determining the *R*-parameter value for this range is impossible due to the insignificant departure of the *S*- and *W*-parameters from their initial values.

There is no substantial difference in the mechanism of annealing of the Fe–Ni–P sample irradiated at 423 K and the sample irradiated at 270 K. Similar to Fe–Ni alloy, the decrease of *S*-parameter in the sample irradiated at 573 K starts at reaching the annealing temperature above 650 K.

3.2. Alloys residual resistivity as a function of fluence and annealing temperature

Presented in Fig. 4(a) are changes in the resistivity for the alloys irradiated at 270, 423, 573 K, respectively, as a function of the electron fluence. The attention is drawn to the high-resistivity growth rate (2.5–20%, depending on the irradiation temperature). It is known [11] that in austenitic alloys the increase of the residual resistivity per Frenkel pair, ρ_F, is about 100 nΩ m at.%$^{-1}$. According to the estimate, at the fluence of 5×10^{22} m^{-2}, the damage of not more than 6×10^{-4} displacement per atom occurs. Therefore, the maximum increase of the resistivity in alloys (at specific resistivity $\rho_0 \approx 400$ nΩ m) due to the accumulation of radiation-induced defects shall be expected to be within 1.5%.

In concentrated alloys, the resistivity growth depends not on the accumulation of defects only, but on the structural-phase transformation as well, particularly on the processes of short-range (local) ordering. Changes of local-atomic order in the alloys are the most probable reason for the significant resistivity growth under irra-

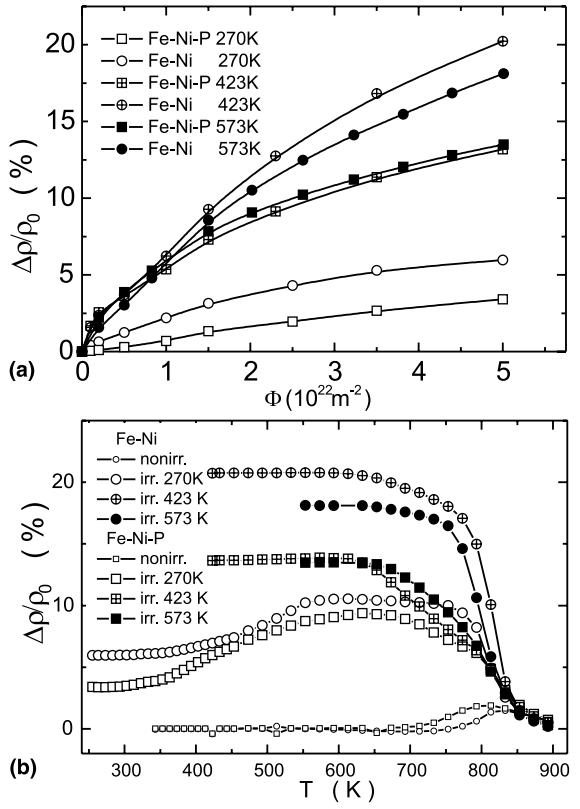

Fig. 4. Relative residual resistivity increase of Fe–Ni, Fe–Ni–P alloys versus irradiation fluence at 270, 423, 573 K, respectively (a); isochronal annealing of the resistivity in 5×10^{22} m^{-2} electron-irradiated and unirradiated alloys (b).

diation. The setting process of the equilibrium state in short-range ordering at the given temperature depends on point defects concentration and their diffusion mobility. It was established in papers [11] dedicated to systematic investigation of Fe–Cr–Ni austenitic alloys that growth of ρ is proportional to the jump number n of migrating point defects. In the case of local processes, the value of n is small, and resistivity drop is similar to that in pure metals. On the other hand, in the case of long-range migration of defects (vacancies and IAs), the effect of ordering prevails, the result being the growth of ρ. It should be noted that in the course of migration the contribution of IAs to the ordering will take effect only at their elementary jumps being able to ensure the atomic exchange. It therefore follows from the obtained data that already at 270 K there takes place migration of defects, which is in agreement with the positron annihilation data.

With the temperature rise, the rate increasing of the residual resistivity becomes substantially greater. It was shown in [17] that after the irradiation with electrons at 523 K, the invar effect in Fe–Ni alloy disappears, and two phases, that is, FeNi and Fe_3Ni, emerge in the alloy. Probably, the high rate of the resistivity growth after the irradiation in this case is caused by the transformation process in Fe–Ni alloy.

In phosphorus-doped alloys, the resistivity growth is partly suppressed. Such effect of phosphorus is characteristic of all the irradiation temperatures.

The curves of resistivity change in the course of the isochronal annealing of alloys irradiated at different temperatures are shown in Fig. 4(b). Such resistivity changes in the course of the isochronal annealing may be conventionally divided into three temperature ranges:

1. 270–400 K. Insignificant increase $\Delta\rho/\rho_0$ is observed, being more noticeable in Fe–Ni–P alloy;
2. 400–600 K. Significant increase $\Delta\rho/\rho_0$ is observed in both alloys, noticeably exceeding the residual resistivity increase after the irradiation;
3. 600–900 K. Drop of $\Delta\rho/\rho_0$ to practically the initial value.

For alloys irradiated at elevated temperatures, the value of the resistivity is constant up to 650 K, with its further continuous decrease to the initial value. According to the phase diagram [17], at temperatures over 650 K, Fe–Ni alloy becomes single phase, i.e., during the isochronal annealing homogenizing of samples must be taking place.

In samples of non-irradiated alloys, the resistivity growth is observed at 700–800 K with subsequent return to the initial value in the region of 850–900 K. It thus follows that at temperatures above 700 K the contribution of thermal vacancies to the diffusion processes in the alloys prevails.

4. Discussion

4.1. Irradiation at 270 K

As shown in Section 3.1, at the irradiation temperature of 270 K, vacancies are already mobile and capable of forming small three-dimensional vacancy clusters. The processes of vacancy clustering occur both in Fe–Ni and in Fe–Ni–P. However, the cluster structure is different in these two alloys. The R-parameter values are lower in Fe–Ni–P than that in Fe–Ni (see Fig. 2). In the general case, values of R-parameter depend on the structure of vacancy clusters and their chemical surrounding [10]. Since in both alloys there are realized three-dimensional configurations of clusters (the S-parameter values are substantially higher than S_v), it may be supposed that vacancies interact with atoms of phosphorus serving as cluster nucleation centers. Decoration of vacancy clusters with phosphorus atoms (3sp-element) in the 3d-matrix leads to the decrease of W-parameter, in line with the increase of $|\Delta W|$ and the

decrease of the *R*-parameter. The fact of decoration is best visualized in the so-called 'ratio curves' [9]. In Fig. 5(a) the ACAR spectra (high-momentum part) of the irradiated Fe–Ni and Fe–Ni–P alloys are shown in comparison with the initial Fe–Ni alloy spectrum. All spectra were preliminarily normalized to the same area. Positron capture by a vacancy cluster leads to the localization of the positron wave function. Superimposition of the wave function of a trapped positron on the ion core electron function diminished. The result is the decrease of the coincidence count rate in the high-momentum part of the ACAR spectrum for the irradiated Fe–Ni alloy. The abrupt dip of the coincidence count rate in the case of Fe–Ni–P is connected with the presence of a phosphorus atom (or atoms) in the immediate neighborhood of the cluster. In this case, positrons annihilate with 2sp-electrons of phosphorus, the probability of this process being low (as compared with 3d-electrons) due to the strong Coulomb repulsion of a positron by a nucleus [8].

Thus the ratio curves analysis shows that vacancies migrate and interact with phosphorus atoms, forming vacancy–phosphorus clusters already at 270 K. The conclusion made in [5,6] on phosphorus atoms restricting substantially (up to about 500 K) the mobility of vacancies in austenitic alloys is not confirmed.

Vacancy–phosphorus clusters in Fe–Ni–P alloy were found to be less thermally stable than vacancy clusters in Fe–Ni, probably due to a more fine-dispersed structure. Fine-dispersed structure is formed at the expense of phosphorus atoms serving as cluster nucleation centers. Dissociation of these clusters starts at 340 K, which is testified to by both the decrease of *S*-parameter value (see Fig. 3(b)) and the increase of the resistivity (see Fig. 4(b)). Long-range migration of vacancies which are released from dissociated clusters stimulates the processes of short-range ordering. The energy of dissociation of vacancy–phosphorus clusters is (1.1 ± 0.1) eV.

In Fe–Ni alloy the dissociation of vacancy clusters begins at the annealing temperatures above 420 K. The energy of dissociation is (1.6 ± 0.1) eV. Along with the dissociation process of clusters in Fe–Ni alloy, there take place the processes of coagulation. At the annealing temperature above 600 K the largest clusters get transformed to vacancy loops. Loops formation at $\approx$600 K is testified to by *R*-parameter drop, as well as by the absence of the resistivity change. It is clear that transformation of three-dimensional clusters into loops is not linked with the long-range vacancy migration.

It should be noted that Fe–Ni–P alloy also has a stage of dissociation of clusters with the energy of 1.6 eV. In their structure and energy characteristics these clusters are close to those in Fe–Ni alloy. But in the dissociation of clusters in Fe–Ni–P alloy the disappearance processes of released vacancies are intensified. This is judged upon by a lower *S*-parameter value in Fe–Ni–P sample subjected to the isochronal annealing to 623 K (Fig. 6). Thus in the alloy with the addition of phosphorus there are formed additional recombination centers or sinks, whose nature will be discussed below. The presence of additional recombination centers in Fe–Ni–

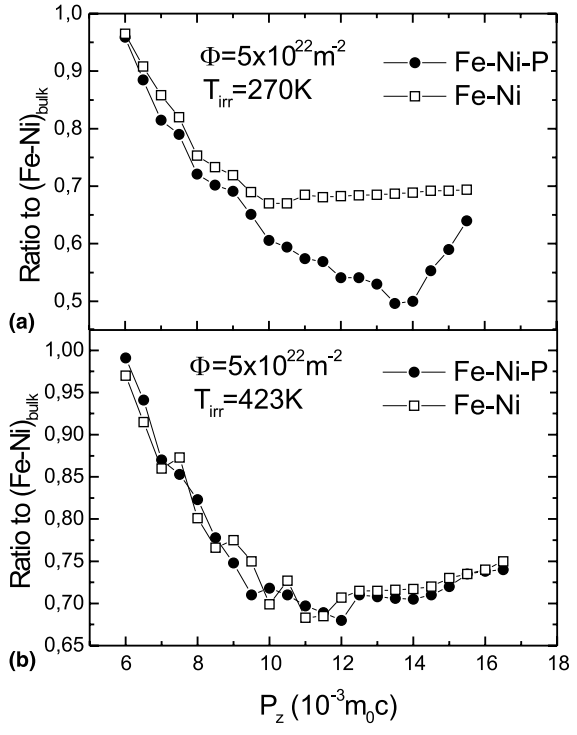

Fig. 5. Ratio curves of the ACAR spectra of Fe–Ni, Fe–Ni–P alloys after irradiation at 270 K (a) and at 423 K (b) with respect to that of bulk Fe–Ni.

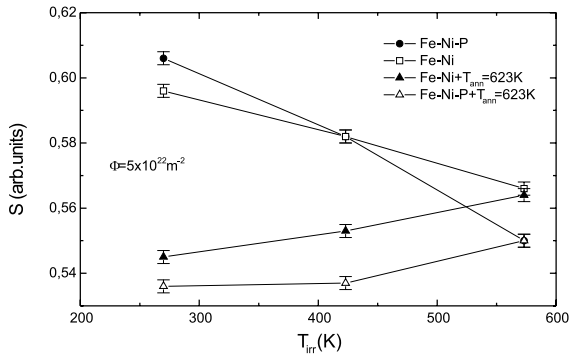

Fig. 6. *S*-parameter variation versus irradiation temperature in Fe–Ni, Fe–Ni–P alloys after electron irradiation and subsequent isochronal annealing at 623 K, respectively.

P leads to partial suppression of vacancy loop formation at ≈600 K.

4.2. Irradiation at elevated temperatures

As it was noted in Section 3.1.1, at elevated irradiation temperatures, with the IA and vacancies being mobile, the processes of their disappearance either as a result of mutual recombination or due to their absorption on sinks are intensified. Indeed, with the irradiation temperature rise, concentration of the accumulated vacancy-type defects drops in both alloys, which is testified to by lowering of the *S*-parameter value shown in Fig. 6.

After the irradiation at 423 K, the *S*-parameter values in both alloys coincide, the ratio curves, also, show no difference (see Fig. 5(b)), that is, no vacancy–phosphorus interaction is observed. Thus a conclusion may be made that at the irradiation temperature of 423 K clusters decorated with phosphorus atoms cease to be formed.

At the irradiation temperature of 573 K, two-dimensional vacancy accumulations vacancy loop nucleation centers are formed in both alloys. But the concentration of such accumulation is considerably lower in Fe–Ni–P (see Fig. 6). As it was noted before, additional recombination centers are formed in Fe–Ni–P, strongly affecting the processes of defect accumulation and annealing.

Let us discuss the behavior of these centers. The behavior of additional recombination centers related to the effect of point defect capture on impurity atoms was theoretically substantiated in [18]. We have shown in Section 4.1 that vacancies interact with phosphorus atoms. As a result of such interaction, clusters decorated with phosphorus atoms are formed. However, the vacancy–phosphorus interaction is weak and exerts no considerable influence on vacancy supersaturation at the irradiation temperature above 400 K. It would be reasonable to suppose that in Fe–Ni alloy phosphorus interacts with IAs. The agglomerates of IA with phosphorus in Fe–Ni act as efficient centers of vacancy recombination. This effect is the most pronounced at elevated irradiation and annealing temperatures, when the IA agglomerates in Fe–Ni have already dissociated and the agglomerates of IAs decorated with phosphorus atoms in Fe–Ni–P have undergone practically no decrease. Indeed, it was shown in [5,6] that in austenitic Fe–Cr–Ni alloys phosphorus atoms strongly interact with IA and serve as centers of the interstitial loop generation. Addition of phosphorus results in the increase of the loop density and their thermal stability at temperatures of up to ≈600 K. Radiation-induced formation of phosphides [3,19], which will also act as additional sinks for vacancies, is another consequence of interstitial–phosphorus interaction.

5. Conclusions

1. It has been shown that vacancies in Fe–36% Ni alloy are mobile at room temperature.
2. Formation of vacancy clusters decorated with phosphorus atoms in Fe–36% Ni–0.1% P alloy at the irradiation temperature of 270 K has been revealed. This is a result of the interaction between vacancies and phosphorus atoms. However vacancy–phosphorus interaction has but a weak effect on vacancy supersaturation at elevated irradiation temperatures.
3. Vacancy supersaturation in Fe–36% Ni–0.1% P alloy at the irradiation temperature of 573 K is suppressed as a result of the interaction between IA and phosphorus atoms.
4. Long-range migration of defects in alloys induces the processes of short-range ordering; and, at elevated irradiation temperatures, the processes of transformation.
5. It has been shown in this paper that high sensitivity of the positron annihilation method allows to obtain the information on vacancy supersaturation of nuclear materials at the early stages of radiation damage development (10^{-4}–10^{-3} dpa).

Acknowledgements

This study has been financially supported by the Program for Leading Research Schools Support (Project No 00-15-96581).

References

[1] G. Gessel, A.F. Rowcliffe, in: M.L. Bleiberg, J.W. Bennett (Eds.), Radiation Effects in Breeder Reactor Structural Materials, TMS-AIME, 1977, p. 431.
[2] F.A. Garner, H.R. Brager, J. Nucl. Mater. 133&134 (1985) 511.
[3] E.H. Lee, P.J. Mariasz, A.F. Rowcliffe, in: J.R. Holland, et al. (Eds.), Phase Stability During Irradiation, TMS-AIME, 1980, p. 191.
[4] F.A. Garner, W.G. Wolfer, J. Nucl. Mater. 102 (1981) 143.
[5] H. Watanabe, A. Aoki, H. Murakami, T. Muroga, N. Yoshida, J. Nucl. Mater. 155–157 (1988) 815.
[6] H. Watanabe, A. Aoki, T. Muroga, N. Yoshida, J. Nucl. Mater. 179–181 (1991) 529.
[7] D. Huguenin, P. Moser, F. Vanoni, J. Nucl. Mater. 169 (1989) 73.
[8] M. Alatalo, H. Kauppinen, K. Saarinen, M.J. Puska, J. Makinen, P. Hautojarvi, R.M. Nieminen, Phys. Rev. B 51 (1995) 4176.
[9] S. Szpala, P. Asoka-Kumar, B. Nielsen, J.P. Peng, S. Hayakawa, K.G. Lynn, H.-J. Gossmann, Phys. Rev. B 54 (1996) 4722.

[10] V.L. Arbuzov, S.E. Danilov, A.P. Druzhkov, Phys. Status Solidi (a) 162 (1997) 567.
[11] C. Dimitrov, O. Dimitrov, J. Phys. F 14 (1984) 793.
[12] R.W. Siegel, Ann. Rev. Mater. Sci. 10 (1980) 393.
[13] S. Mantl, W. Triftshauser, Phys. Rev. B 17 (1978) 1645.
[14] V.L. Arbuzov, A.P. Druzhkov, S.M. Klotsman, Fiz. Khim. Obrab. Mater. 1 (1991) 24 in Russian.
[15] S.M. Myers, P. Nordlander, F. Besenbacher, J.K. Norskov, Phys. Rev. B 33 (1986) 854.
[16] A.C. Damask, G.J. Dienes, Point Defects in Metals, Gordon and Breach, London, 1963.
[17] A. Chamberod, J. Laugier, J.M. Penisson, J. Magn. Magn. Mater. 10 (1979) 139.
[18] L.K. Mansur, J. Nucl. Mater. 83 (1979) 109.
[19] H. Watanabe, T. Muroga, N. Yoshida, J. Nucl. Mater. 271&272 (1999) 381.